## *Electronic Supplementary Information*

# Plutonium(IV) complexation by diglycolamide ligands—coordination chemistry insight into TODGA–based actinide separations

**Sean D. Reilly, Andrew J. Gaunt,* Brian L. Scott, Giuseppe Modolo, Mudassir Iqbal, Willem Verboom* and Mark J. Sarsfield**

**General Experimental Details.** *Caution! All plutonium chemistry (weapons grade isotopic composition, obtained from internal sources at Los Alamos National Laboratory) was conducted inside specialist radiological facilities designed for the safe handling and manipulation of high specific-activity $\alpha$-particle emitting radionuclides.* The TMDGA and TEDGA ligands were prepared by reaction of diglycolyl chloride with the appropriate amine according to G. Tian, L. Rao, S. J. Teat and G. Liu, *Chem. Eur. J.*, 2009, **15**, 4172-4181. The procedure was modified to use THF instead of dioxane as a solvent.
N,N,N',N'-tetraoctyl diglycolamide (TODGA) was synthesised employing diglycolyl chloride and dioctylamine as starting materials in accordance to the literature (Y. Sasaki and R. Choppin, *Anal. Sci.,* 1996, **12**(2), 225-230) followed by purification. The identity and purity of the product was confirmed by $^1$H-NMR and $^{13}$C-NMR and was shown to be >99% pure.

**Vis-NIR and FT-IR data collection details**. Solution electronic absorption spectra were collected in quartz cuvettes at room temperature using a Varian Cary 6000i UV-vis-NIR spectrophotometer with a 0.3 nm spectral bandwidth. Solid diffuse reflectance spectra were collected using a Varian Cary 6000i with installed Internal Diffuse Reflectance Accessory. Crystals of $[Pu^{IV}(TMDGA)_3](NO_3)_4\cdot MeCN$ were ground into a powder and loaded into a sealed glass sample holder in order to obtain the diffuse reflectance spectrum. FT-IR spectra were collected using a Nicolet 6700 spectrometer. A nujol mull of solid $[Pu^{IV}(TMDGA)_3](NO_3)_4\cdot MeCN$ was prepared and placed between two KBr discs that were then taped together to contain the radioactive material so that the FT-IR spectrum could be obtained.

**Synthesis of crystalline $[Pu^{IV}(TMDGA)_3](NO_3)_4\cdot EtOH$:** Aqueous Pu(IV)/$HNO_3$ solution (12 µL, 6.0 µmol Pu) was added to 2.00 mL of EtOH (200 proof). The spectrum of this clear green Pu(IV) / EtOH solution was recorded (Fig S1). N,N,N',N'-tetramethyl diglycolamide (TMDGA, 11.8 mg, 62.7 µmol) was dissolved in 400 µL of EtOH. This TMDGA solution was added in aliquots to the above Pu solution and the vis-NIR spectrum was recorded after each addition. A total of 395 µL of this TMDGA solution was added. The final solution was allowed to slowly evaporate. Diffraction-quality crystals were observed in the concentrated solution one month later. The crystal structure was obtained from these crystals, and found to be $[Pu^{IV}(TMDGA)_3](NO_3)_4\cdot EtOH$

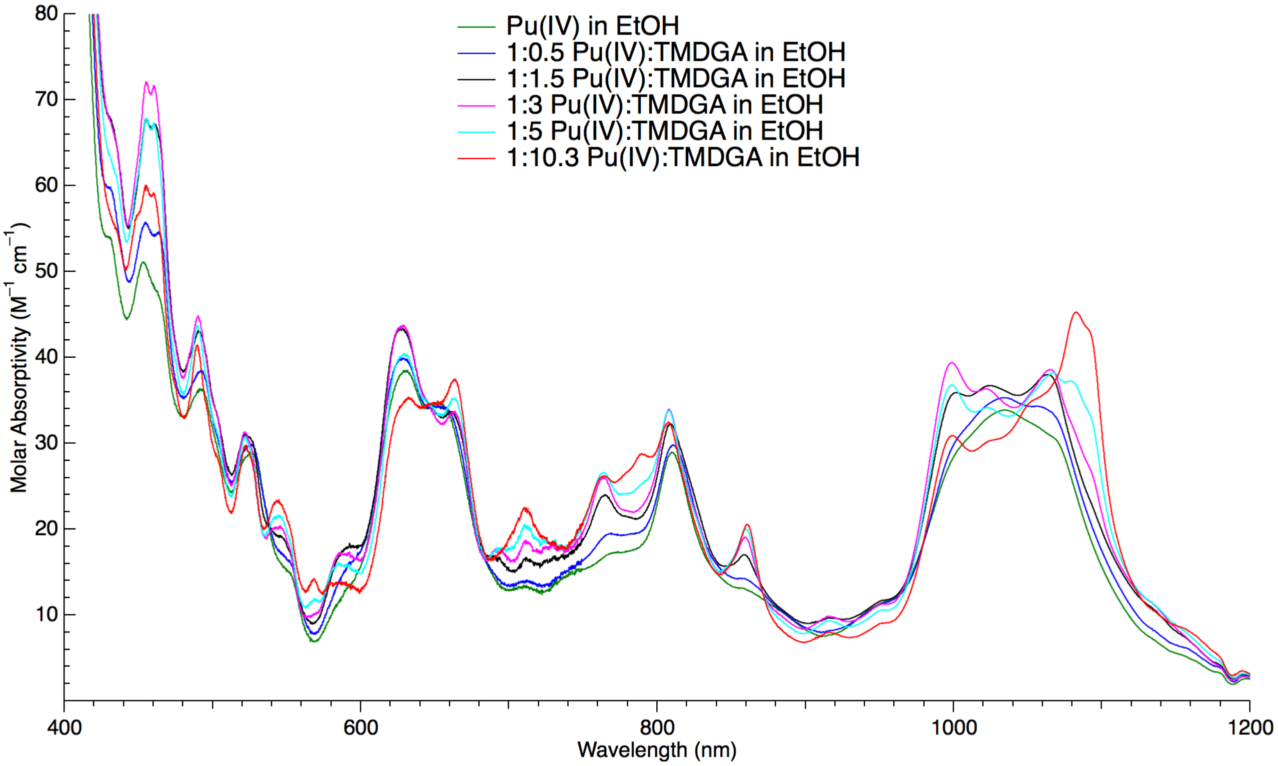

Fig S1. Solution electronic absorption spectra of 2.5–3.0 mM Pu(IV) in EtOH as a function of added TMDGA. The TMDGA was completely soluble in EtOH and was added as a 0.157 M solution in EtOH. Evaporation of the final solution yielded single crystals with the structure $[\mathrm{Pu^{IV}(TMDGA)_3}](\mathrm{NO_3})_4\cdot\mathrm{EtOH}$.

**Synthesis of crystalline [Pu$^{IV}$(TMDGA)$_3$](NO$_3$)$_4$·MeCN:** Solid [N(*n*-Bu)$_4$]$_2$Pu(NO$_3$)$_6$ was dissolved in MeCN and the vis–NIR absorption spectrum was recorded (Fig S2). This green Pu(NO$_3$)$_6^{2-}$/MeCN solution (860 µL, 27.8 µmol Pu$^{IV}$) was added to solid TMDGA (15.9 mg, 84.5 µmol) — the TMDGA readily dissolved as the Pu was added. The vis–NIR spectrum of the resulting solution was recorded (Fig S2). This solution was left to evaporate slowly over 2 days to give orange crystals. The crystal structure was obtained from these crystals, and found to be [Pu$^{IV}$(TMDGA)$_3$](NO$_3$)$_4$·MeCN.
It was subsequently found that identical crystals could be grown overnight by vapor diffusion of Et$_2$O into a 1:3 Pu$^{IV}$:TMDGA MeCN solution. In a typical reaction, 3 equiv of a TMDGA solution in MeCN (289 µL, 79.4 µmol) was titrated into a green Pu(NO$_3$)$_6^{2-}$/MeCN solution (710 µL, 26.6 µmol Pu$^{IV}$). Vis–NIR spectra of the reaction solution were collected over the course of the titration (Fig S3). Vapor diffusion of the final solution with Et$_2$O yielded solid crystals of [Pu(TMDGA)$_3$](NO$_3$)$_4$·MeCN (47% yield).

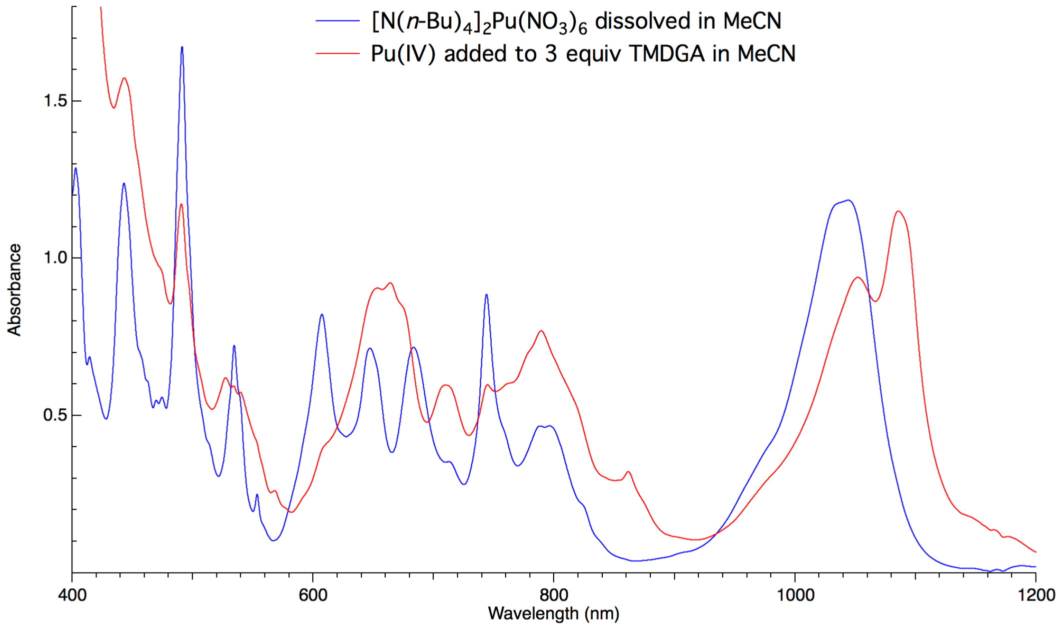

Fig S2. Solution electronic absorption spectra of 32.3 mM [N(*n*-Bu)$_4$]$_2$Pu(NO$_3$)$_6$ dissolved in MeCN (blue) and 1:3 Pu$^{IV}$:TMDGA after combining in MeCN (red).

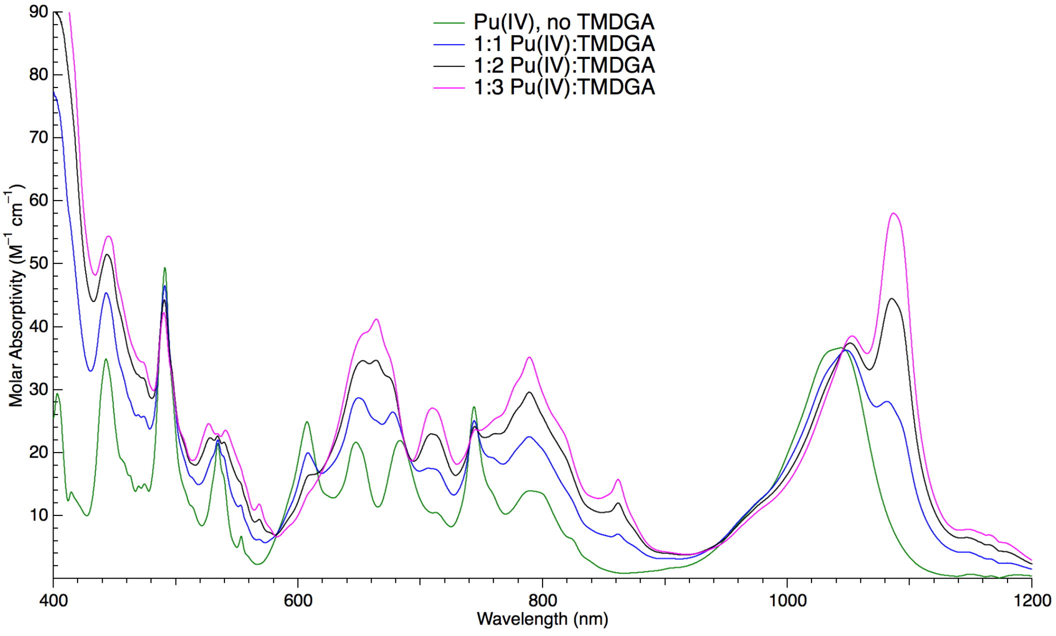

Fig S3. Solution electronic absorption spectra of 26.6–37.5 mM Pu(IV) in MeCN as a function of added TMDGA. The initial Pu(IV) solution was prepared by dissolving solid [N(*n*-Bu)$_4$]$_2$Pu(NO$_3$)$_6$ in MeCN, and the TMDGA was added as a 0.275 M solution in MeCN.

**Single-crystal X-ray Diffraction Collection Details.** Pu containing single crystals were coated in paratone-N oil and mounted inside a 0.5 mm capillary tube, which was sealed with hot capillary wax. The sealed capillary was coated with a thin film of acrylic in ethyl acetate (Hard as Nails®) to provide structural integrity and additional containment. The capillary was placed on a Bruker Platform diffractometer with 1k CCD, and cooled to 140 K using a Bruker Kryoflex cryostat. The instrument was equipped with a sealed, graphite monochromatized MoKα X-ray source (λ= 0.71073 Å). Data collection and initial indexing and cell refinement were handled using SMART software (version 5.632, **2005**, Bruker AXS, Inc., Madison, Wisconsin 53719). Frame integration, including Lorentz-polarization corrections, and final cell parameter calculations were carried out using SAINT+ software (version 6.45, **2003**, Bruker AXS, Inc., Madison, Wisconsin 53719). The data were corrected for absorption using the SADABS program (version 2.05, **2002**, George Sheldrick, University of Göttingen, Germany). Decay of reflection intensity was monitored *via* analysis of redundant frames. The structure was solved using Direct methods and difference Fourier techniques. Hydrogen atoms were idealized. The final refinement included anisotropic temperature factors on all non-hydrogen atoms. Structure solution, refinement, and materials for publication were performed using SHELXTL Version 6.10, **2001**, Bruker AXS, Inc., Madison, Wisconsin 53719).

SQUEEZE was applied to the ethanol solvate to account for lattice voids resulting in the outcome of one lattice ethanol molecule per complex. In the case of the acetonitrile solvate, one MeCN molecule was found in the lattice and refined.

**Crystal data for [Pu$^{IV}$(TMDGA)$_3$](NO$_3$)$_4$·EtOH:** $C_{26}H_{54}N_{10}O_{22}Pu$, $M$ = 1097.77, monoclinic, $a$ = 21.121(5), $b$ = 12.830(3), $c$ = 19.842(5) Å, $\alpha$ = 90.00, $\beta$ = 104.811(3), $\gamma$ = 90.00°, $V$ = 5198(2) Å$^3$, $T$ = 140(2) K, space group $C2/c$, $Z$ = 4, $\mu$ = 1.342 mm$^{-1}$, reflections collected/independent = 23624/4926 ($R_{\mathrm{int}}$ = 0.0759), $R_1(I > 2\sigma(I))$ = 0.0698, and $wR_2(I > 2\sigma(I))$ = 0.1735.

**Crystal data for [Pu$^{IV}$(TMDGA)$_3$](NO$_3$)$_4$·MeCN:** $C_{26}H_{51}N_{11}O_{21}Pu$, $M$ = 1092.75, monoclinic, $a$ = 10.2980(16), $b$ = 37.077(6), $c$ = 10.7859(17) Å, $\alpha$ = 90.00, $\beta$ = 95.598(2), $\gamma$ = 90.00°, $V$ = 4098.6(11) Å$^3$, $T$ = 140(2) K, space group $P2_1/c$, $Z$ = 4, $\mu$ = 1.701 mm$^{-1}$, reflections collected/independent = 40321/7780 ($R_{\mathrm{int}}$ = 0.0307), $R_1(I > 2\sigma(I))$ = 0.0886, and $wR_2(I > 2\sigma(I))$ = 0.1622.

**Table S1.** Selected bond distances (Å) and angles (°) for [Pu$^{IV}$(TMDGA)$_3$](NO$_3$)$_4$·EtOH.

| | | | |
|---|---|---|---|
| Pu(1)–O(1) | 2.317(6) | O(1)–Pu(1)–O(3) | 125.6(2) |
| Pu(1)–O(2) | 2.504(6) | O(4)–Pu(1)–O(4A) | 126.4(3) |
| Pu(1)–O(3) | 2.297(6) | | |
| Pu(1)–O(4) | 2.284(7) | | |
| Pu(1)–O(5) | 2.437(8) | | |

**Comparisons of vis–NIR diffuse reflectance spectrum of crystalline [Pu$^{IV}$(TMDGA)$_3$](NO$_3$)$_4$·MeCN to Pu(IV)–TMDGA solution spectra:**

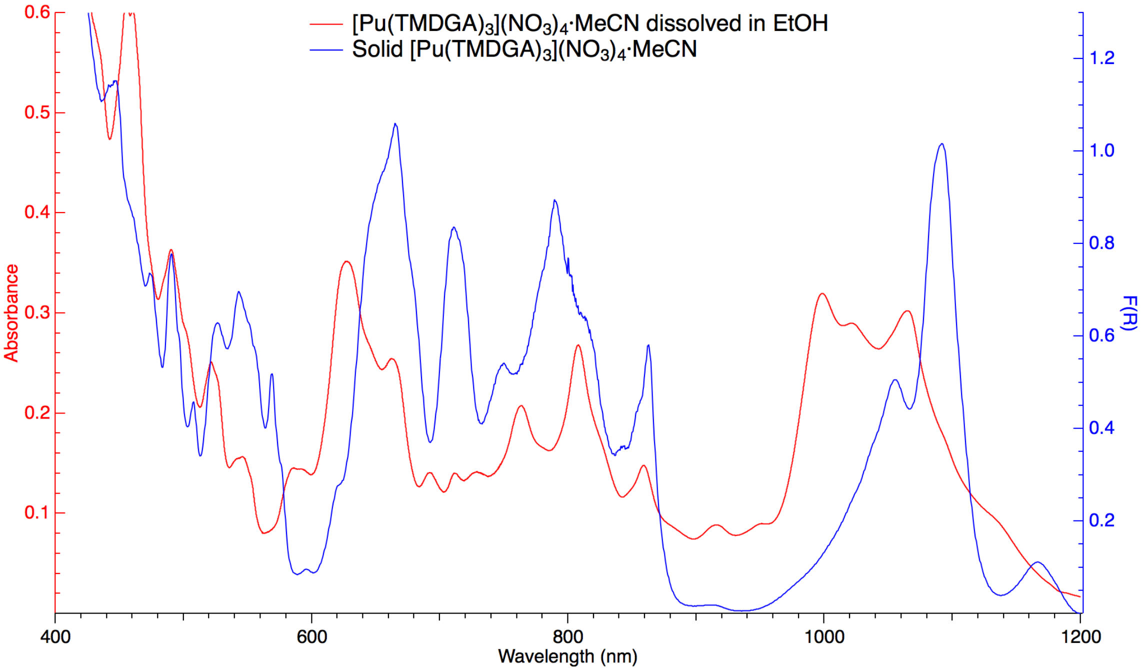

Fig S4. Vis–NIR diffuse reflectance spectrum of solid [Pu$^{IV}$(TMDGA)$_3$](NO$_3$)$_4$·MeCN (blue spectrum, right axis). The solution electronic absorption spectrum of the above crystals dissolved in EtOH (red spectrum, left axis) is shown for comparison. The spectra suggest that the Pu(TMDGA)$_3$$^{4+}$ complex partially dissociates in EtOH, contrary to what was observed for MeCN (see Fig 4 in main communication). The red spectrum in this figure closely resembles that of the 1:3 Pu(IV):TMDGA solution in EtOH shown in Fig S1, which also suggests that Pu(TMDGA)$_3$$^{4+}$ is not the only complex present at that point in the Fig S1 titration.

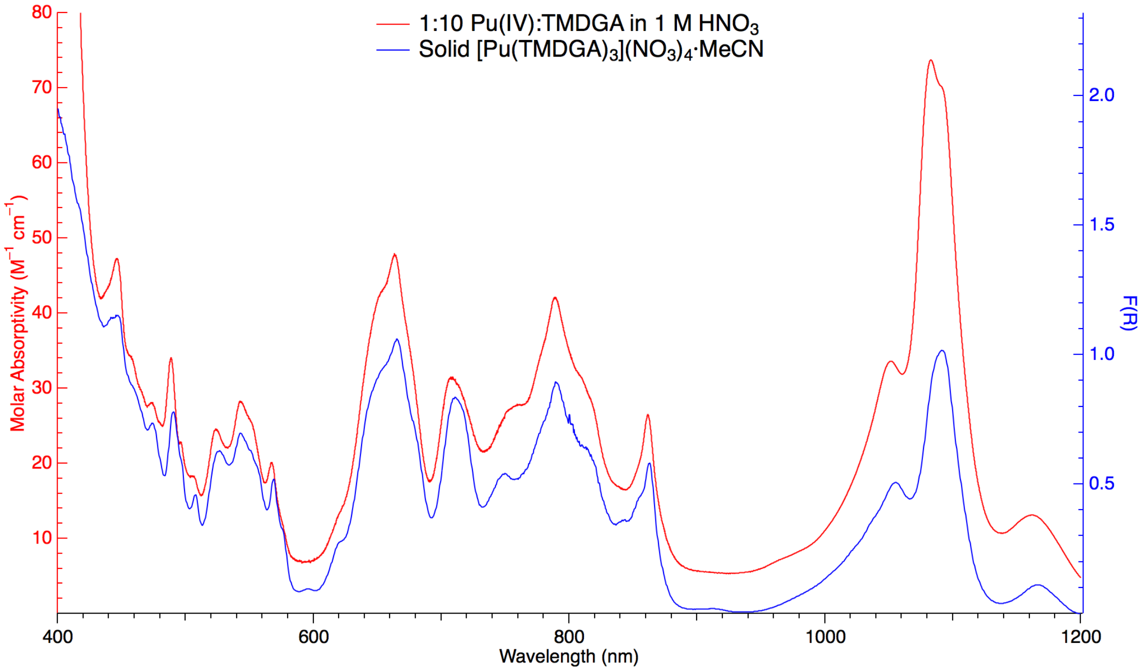

Fig S5. Vis–NIR diffuse reflectance spectrum of solid [Pu$^{IV}$(TMDGA)$_3$](NO$_3$)$_4$·MeCN (blue spectrum, right axis). The solution electronic absorption spectrum of 1:10 Pu(IV):TMDGA in aqueous 1 M HNO$_3$ is show for comparison (red spectrum, left axis). The close resemblance of the two spectra suggests that Pu(TMDGA)$_3$$^{4+}$ is the dominant species with the solution conditions stated above.

**Comparisons of vis–NIR spectra of TODGA, TEDGA and TMDGA titrations of $Pu(NO_3)_6 \cdot 2TBA$ in MeCN:**

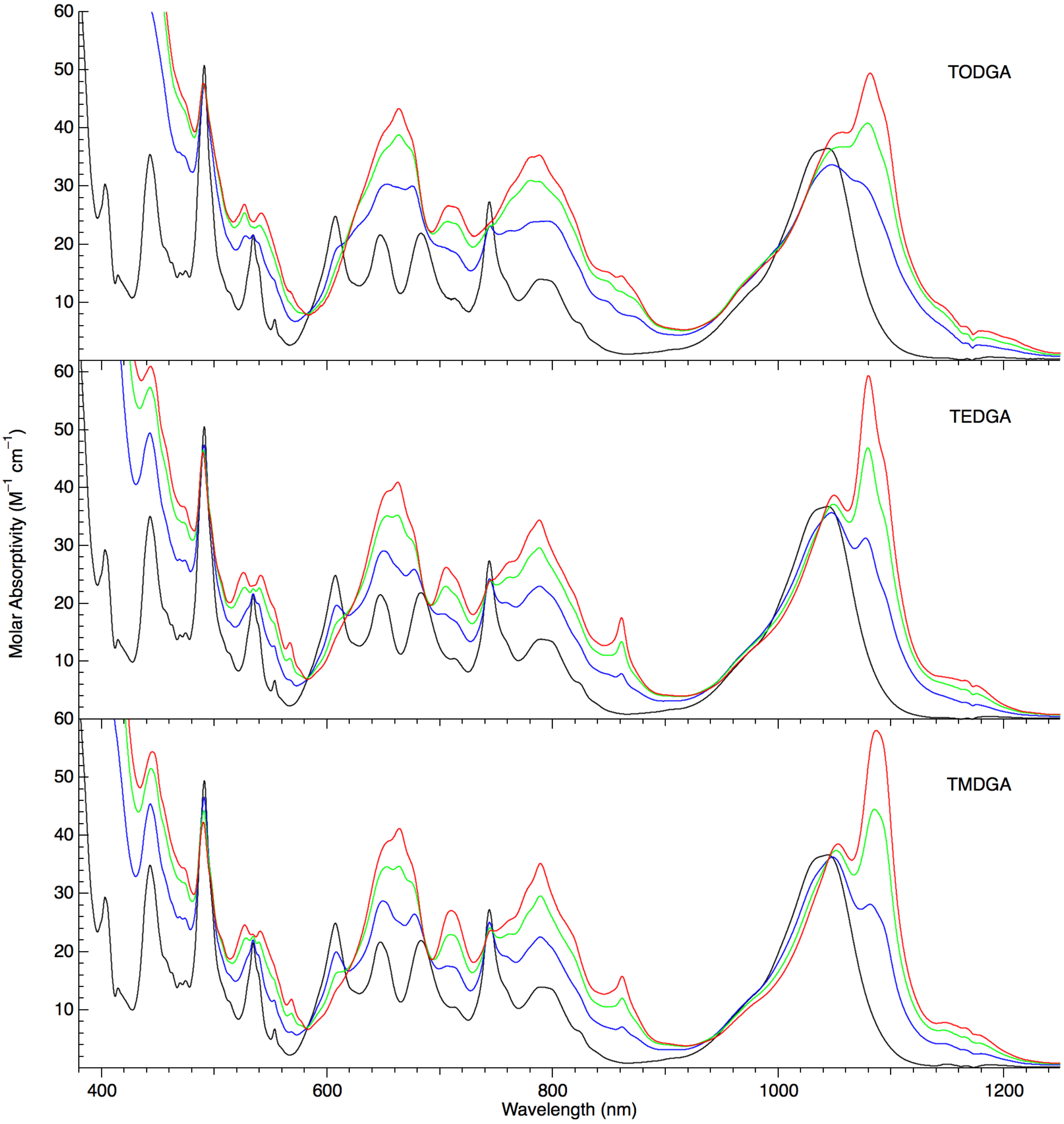

Fig S6. Solution electronic absorption spectra of Pu(IV) in MeCN as a function of added TODGA (top), TEDGA (middle), or TMDGA (bottom). The Pu(IV) concentrations are as follows: 5.3–6.2 mM (TODGA titrn), 12.5–17.5 mM (TEDGA), 26.6–37.5 mM (TMDGA). Equivalents of added DGA ligand: 0 (black), 1.0 (blue), 2.0 (green), 3.0 (red).

**Infrared spectra:**

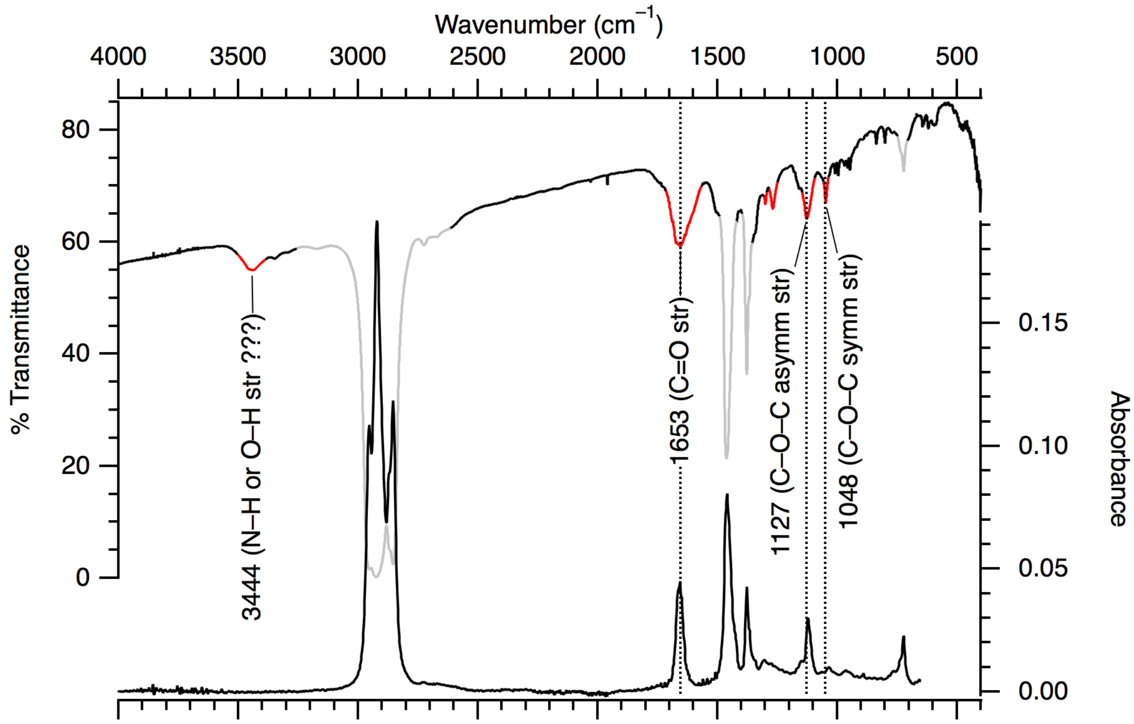

Fig S7. Infrared transmittance spectrum of TMDGA in nujol (left axis). The principal bands are highlighted in red, and the principal bands arising from nujol are "greyed out" (3260–2617, 1487–1419, 1397–1354, 727–680 cm$^{-1}$). The infrared absorbance spectrum of TODGA in kerosene[1] is shown for comparison (right axis).

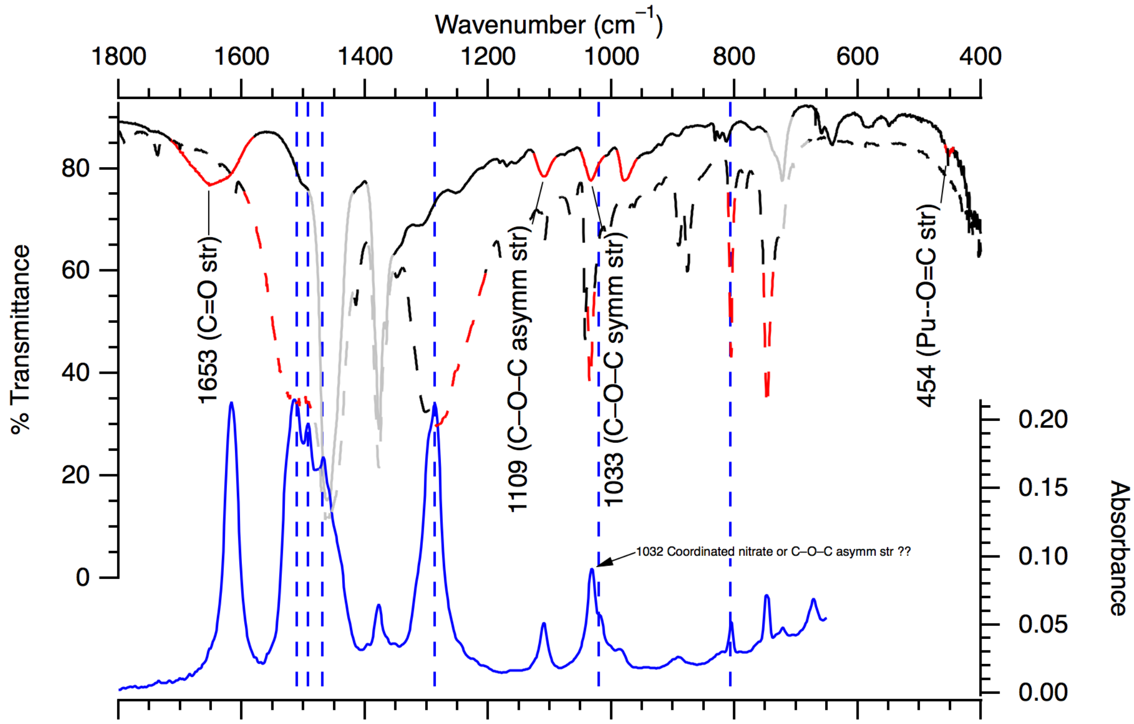

Fig S8. Infrared transmittance spectrum of [Pu$^{IV}$(TMDGA)$_3$](NO$_3$)$_4$·MeCN (left axis, solid line) and [N($n$-Bu)$_4$]$_2$Pu(NO$_3$)$_6$ (left axis, dashed line) in nujol. The principal bands are highlighted in red, and the principal bands arising from nujol are "greyed out" (3260–2617, 1487–1419, 1397–1354, 727–680 cm$^{-1}$). The infrared absorbance spectrum of the "Pu solid washed with Kerosene" [1] is shown for comparison (right axis, blue line). The dashed blue lines indicate the vibrations that Brown et al. attributed to coordinated nitrate.

[1] J. Brown, F. McLachlan, M. Sarsfield, R. Taylor, G. Modolo and A. Wilden, *Solvent Extr. Ion Exch.*, 2012, **30**, 127-141.

**Table S2**. Infrared bands and assignments for TMDGA ligand and Pu(IV)–TMDGA complex $[Pu^{IV}(TMDGA)_3](NO_3)_4 \cdot MeCN$, and comparison with selected related compounds from the literature.

| Compound | Frequency ($cm^{-1}$) and assignment | | | | | | | | Reference |
|---|---|---|---|---|---|---|---|---|---|
| | C=O stretch | C–O–C asymm stretch | C–O–C symm stretch | Nitrate vibrations | | | | | |
| TMDGA | 1653 (broad) | 1127 | 1048 | | | | | | This work |
| TMDGA | 1688 | 1128 | 1051 | | | | | | 2 |
| TMDGA | 1650 | 1135* | 1060* | | | | | | 3 |
| TODGA | 1649 | 1122 | | | | | | | 1 |
| $[Pu(TMDGA)_3](NO_3)_4 \cdot MeCN$ | 1653 (broad) | 1109 | 1033 | | | | | | This work |
| Pu solid washed with kerosene | 1613 | 1110 | | 1510, 1492, 1469 ($\nu_1$) | 1020 ($\nu_2$) | | 1286 ($\nu_4$) | 806 ($\nu_6$) | 1 |
| $UO_2(TMDGA)_2(ClO_4)_2$ | 1631 | 1095 | 1043 | | | | | | 2 |
| $La(TMDGA)_3(ClO_4)_3$ | 1630 | 1130* | 1050* | | | | | | 3 |
| $[N(n\text{-}Bu)_4]_2Pu(NO_3)_6$ | | | | 1512 ($\nu_1$) | 1035 ($\nu_2$) | 747 ($\nu_3$) | 1283 ($\nu_4$) | 806 ($\nu_6$) | 4 |
| $Pu(NO_3)_4(Ph_3PO)_2$ | | | | 1520 ($\nu_1$) | 1032 ($\nu_2$) | | 1295 ($\nu_4$) | 809 ($\nu_6$) | 5 |
| $NaNO_3$ | | | | 1390 ($\nu_3$) | | 720 ($\nu_4$) | | 831 ($\nu_2$) | 6 |

*The authors assign the 1135 and 1130 $cm^{-1}$ bands to a N–$CH_3$ rocking vibration, but it seems likely that this is instead the C–O–C asymmetric stretch. The authors do not explicitly state whether they assign the 1060 and 1050 $cm^{-1}$ bands as symmetric vs asymmetric stretch.

1 J. Brown, F. McLachlan, M. Sarsfield, R. Taylor, G. Modolo and A. Wilden, *Solvent Extr. Ion Exch.*, 2012, **30**, 127-141.
2 G. Tian, L. Rao, S. J. Teat and G. Liu, *Chem.--Eur. J.*, 2009, **15**, 4172-4181.
3 C. Premlatha and S. Soundararajan, *J. Inorg. Nucl. Chem.*, 1980, **42**, 1783-1786.
4 The synthesis and characterization of $[N(n\text{-}Bu)_4]_2[Pu(NO_3)_6]$ will be reported elsewhere.
5 D. L. Plymale, *J. Inorg. Nucl. Chem.*, 1969, **31**, 236-239.
6 B. M. Gatehouse, S. E. Livingstone and R. S. Nyholm, *J. Chem. Soc.*, 1957, 4222-4225.

**Additional Pu(IV)–TMDGA solution titration vis–NIR spectra:**

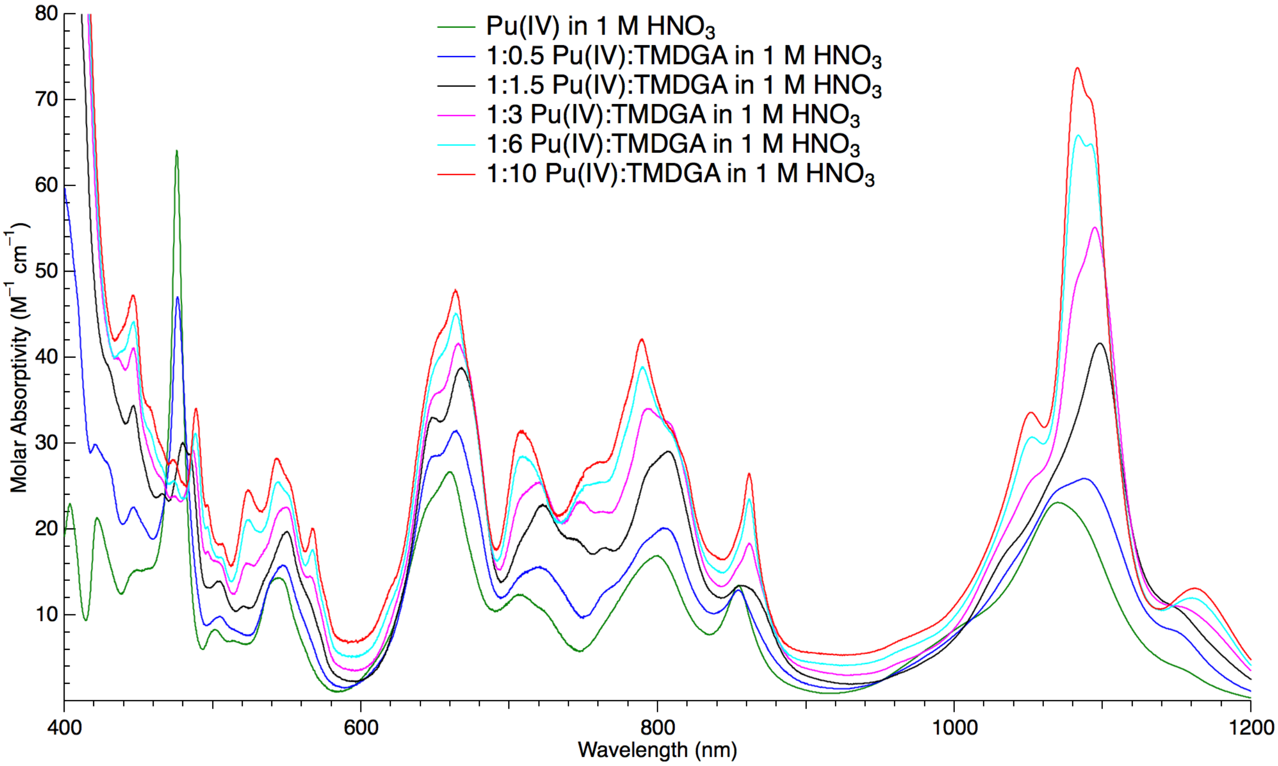

Fig S9. Solution electronic absorption spectra of 5.0–7.4 mM Pu(IV) in aqueous 1 M $HNO_3$ as a function of added TMDGA. The TMDGA was added as a 0.155 M solution in $HNO_3$, but the TMDGA was not completely soluble so the Pu:TMDGA ratio is not highly accurate. There appears to be isosbestic behavior between 0–1.5 equiv TMDGA and between 3–6 equiv TMDGA suggesting the presence of at least two Pu:TMDGA complexes.

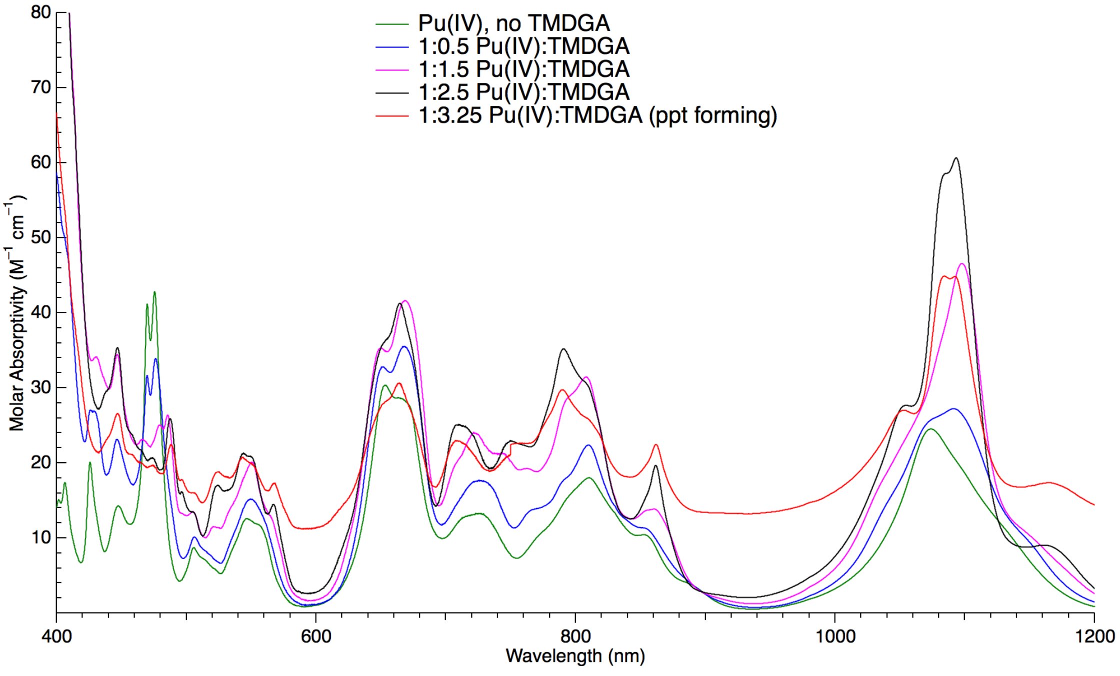

Fig S10. Solution electronic absorption spectra of 6.5–8.6 mM Pu(IV) in aqueous 1 M $HClO_4$ as a function of added TMDGA. The TMDGA was added as a 0.084 M solution in 1 M $HClO_4$, but the TMDGA was not completely soluble so the Pu:TMDGA ratio is not highly accurate. Spectra up to 1.5 equiv added TMDGA are quite similar to those observed for the analogous titration in 1 M $HNO_3$ (Fig S8), but behavior diverges above that. The peak at 791 nm is far more pronounced by 2.5 equiv TMDGA in $HClO_4$, with this spectrum more closely resembling the spectrum of solid $[Pu^{IV}(TMDGA)_3](NO_3)_4\cdot MeCN$ (Fig S4 blue spectrum). A pinkish precipitate began to form soon there after (note elevated baseline at 3.25 equiv TMDGA). This precipitate was not characterized further.

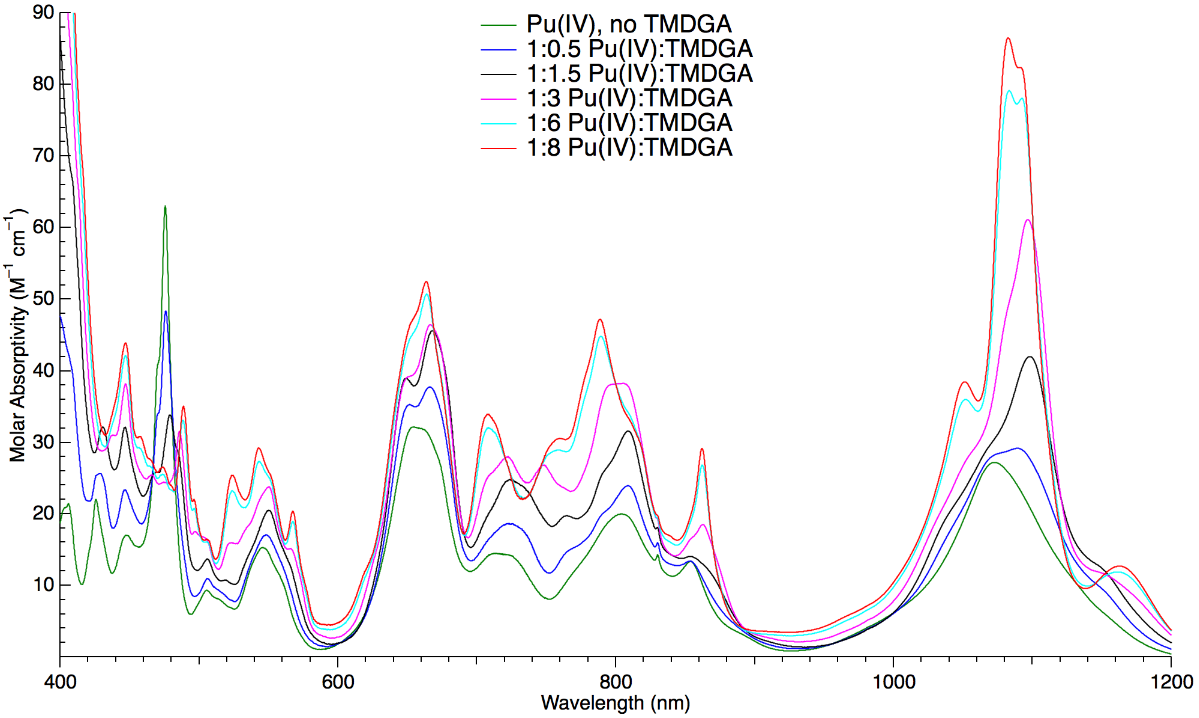

Fig S11. Solution electronic absorption spectra of 5.9–8.6 mM Pu(IV) in aqueous 1 M TfOH as a function of added TMDGA. The TMDGA was added as a 0.151 M solution in 1 M TfOH, but the TMDGA was not completely soluble so the Pu:TMDGA ratio is not highly accurate. There is a trace of Pu(VI) in the Pu(IV) stock solution as indicated by the small peak at 830 nm.

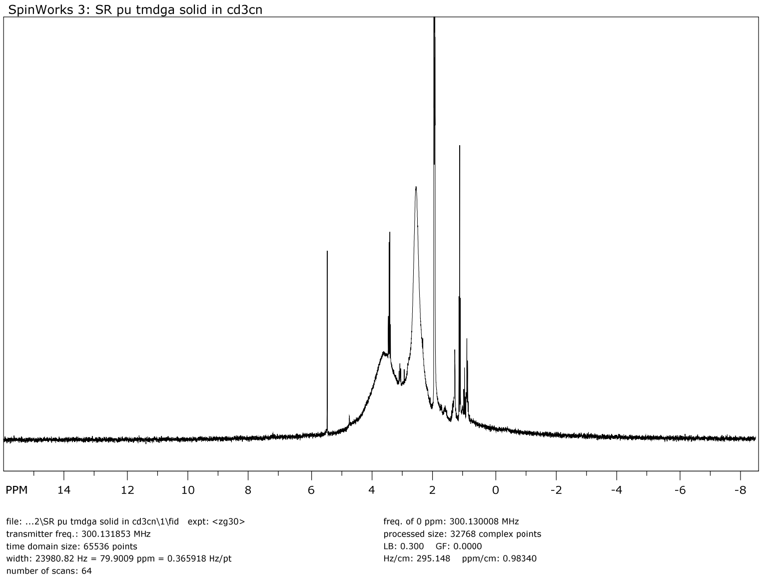

```
file: ...2\SR pu tmdga solid in cd3cn\1\fid   expt: <zg30>
transmitter freq.: 300.131853 MHz
time domain size: 65536 points
width: 23980.82 Hz = 79.9009 ppm = 0.365918 Hz/pt
number of scans: 64

freq. of 0 ppm: 300.130008 MHz
processed size: 32768 complex points
LB: 0.300    GF: 0.0000
Hz/cm: 295.148    ppm/cm: 0.98340
```

Fig S12. $^1$H NMR spectrum of $[Pu(TMDGA)_3](NO_3)_4{\cdot}MeCN$ dissolved in $CD_3CN$. The two broad resonances at 2.6 and 3.6 ppm are attributed to the protons of the coordinated TMDGA ligand to Pu(IV) due to paramagnetic broadening. All of the other resonances can be assigned to common solvent impurities present in the glovebox atmosphere and hence the $CD_3CN$ solvent (G. R. Fulmer, A. J. M. Miller, N. H. Sherdan, H. E. Gottlieb, A. Nudelman, B. M. Stoltz, J. E. Bercaw and K. I. Goldberg, *Organometallics*, 2010, **29**, 2176-2179). These impurities do not affect the assignment of resonances for the Pu-TMDGA complex. The operation of the plutonium glovebox (in which the NMR sample was prepared) at negative pressure precludes any box purging on safety grounds and this can sometimes lead to difficulties in removing solvent vapors from the box atmosphere. The TMDGA ligand dissolved in $CD_3CN$ displayed the same solvent impurities.

.